



## Effect of Porosity Shape, Size and Distribution on Stress Intensity Factors in Spot Welded Joints: A Finite Element Study

Imen Benala<sup>1\*</sup>, Leila Zouambi<sup>2,3</sup>, Farida Bouafia<sup>1,2</sup>, Boualem Serier<sup>3</sup>, Sardar Sikandar Hayat<sup>4</sup>

<sup>1</sup> Smart Structures Laboratory (SSL), University of Ain Temouchent Belhadj Bouchaib, Ain Temouchent 46000, Algeria

<sup>2</sup> LMPM, Mechanical Engineering Department, University of Sidi-Bel-Abbes Djillali Liabes, Sidi-Bel-Abbes 22000, Algeria

<sup>3</sup> Mechanical Engineering Department, University of Relizane Ahmed Zabana, Relizane 48000, Algeria

<sup>4</sup> Department of Physics, International Islamic University, Islamabad 44000, Pakistan

Corresponding Author Email: [imen.benala@univ-temouchent.edu.dz](mailto:imen.benala@univ-temouchent.edu.dz)

<https://doi.org/10.18280/acsm.470304>

### ABSTRACT

**Received:** 22 May 2023

**Accepted:** 5 June 2023

#### Keywords:

*spot welds, stress concentration, fracture mechanics, porosity, finite element analysis, mixed mode fracture*

In this study, the influence of porosity on crack initiation behavior in welded structures subjected to spot welding was investigated. Three-dimensional (3D) finite element analyses were conducted using the ABAQUS finite element software under mechanical stress. The stress intensity factors (SIF) in opening and moving modes were computed employing the finite element technique. A comprehensive analysis of various parameters, including mechanical load, crack size, porosity form, porosity size, porosity-crack interaction, and crack orientation, was carried out. This investigation was approached as a mixed-mode, plane stress, and linear elastic fracture mechanics problem with a focus on the passive voice. The results demonstrated that the stress intensity factor is not only dependent on the magnitude of the applied mechanical loading but also on factors such as crack size, porosity form, defect-defect interaction, and crack orientation. Additionally, it was observed that both the size and form of porosity play a significant role in influencing the stress intensity factors. This research contributes to the understanding of fracture mechanics in welded structures and provides valuable insights for enhancing the structural integrity and reliability of such systems.

## 1. INTRODUCTION

Polluting emission criteria in the automobile sector have driven the development of lightweight vehicles, primarily through the reduction of steel sheet thickness [1]. Spot welding, a process that generates zones of microstructural heterogeneity, is commonly employed to assemble these sheets. Notably, spot welding is considered one of the most efficient methods for joining two or more metal sheets [2]. However, welds often exhibit defects such as porosity, inclusions, and voids [3, 4], which are influenced by factors including the chemical composition of the materials and welding conditions. The weld profile's shape results in high stress concentrations, leading to crack initiation and propagation under static or cyclic loading until the weld bead fractures [3-5]. Consequently, the failure behavior of welded structures has been extensively investigated in recent years.

In this work, the finite element method is utilized for the numerical analysis of a weld joint containing a defect, employing the ABAQUS software [6]. The study is grounded in the theory of linear elastic fracture mechanics. A three-dimensional finite element analysis is conducted to simulate stress distribution around the defect, examining the influence of defect geometrical parameters. The welded structure containing the defect is subjected to uniaxial mechanical loading, and the investigation is extended to consider defect-defect interaction. Steel, treated as an elastic material, is selected as the sample material for this study.

This analysis aims to enhance the understanding of failure

behavior in welded joints containing defects, providing valuable insights for improving the structural integrity and reliability of such systems in the context of the automobile sector's demand for lightweight materials.

## 2. STRESSES AROUND A SPOT WELD

The failure of welded structures has been the subject of numerous researches both experimentally and numerically [7-10]. Without an effective analytical model, interpreting experimental results is difficult. On the other side, numerically based procedures have been successfully applied. The results of these investigations provide clarity on numerous aspects of how welded structures fail. The primary objective of the fracture mechanics of a point resistance welded structure is the determination of the failure parameters, such as notch stresses, stress intensity factors SIF, and the integral J [11]. When tensile loading is applied to a welded structure with a crack, the structure may behave in one of three ways: it may open (mode I), slide (mode II), or exhibit a mixture of the two modes (mixed mode) [1, 12, 13].

The notch between the two thin sheets joined by the weld bead ends in a pointed shape. The origin of this notch is directly related to the welding point and it is considered as an intrinsic crack.

The stress intensity factors SIF in mode I and II are obtained theoretically as a function of the structural stresses [14] developed around the weld point, respectively, by the

following equations:

$$k_I = \frac{\sqrt{3}}{2} (\sigma_{ui} - \sigma_{uo} - \sigma_{li} - \sigma_{lo}) \quad (1)$$

$$k_{II} = 1/4 (\sigma_{ui} - \sigma_{li}) \sqrt{t} \quad (2)$$

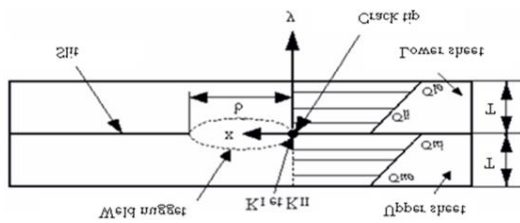


Figure 1. Radial normal stresses [3]

The radial stresses act close to the core of the point of welding ( $x \approx 0$ ) respectively on the inner (i) and outer (o) surfaces of the two upper (u) and lower (l) sheets (Figure 1).

### 3. FINITE ELEMENT MODEL

The behavior of fractures started in the steel matrix and exposed to tensile stresses was examined using the ABAQUS computer code [6], which is based on the finite element approach. Our earlier work [15-17] had successfully used the finite element model, and more recent calculations [4, 18, 19] employing this model's mesh size convergence have validated this. Here, the key elements of the technique are explained. The three-dimensional (3-D) structure under analysis is made of a steel matrix with a weld-related flaw (porosity). This structure has an "a"-sized matrix-initiated crack. Only one-half of the geometry was represented because of the geometry's symmetry (see Figure 2).

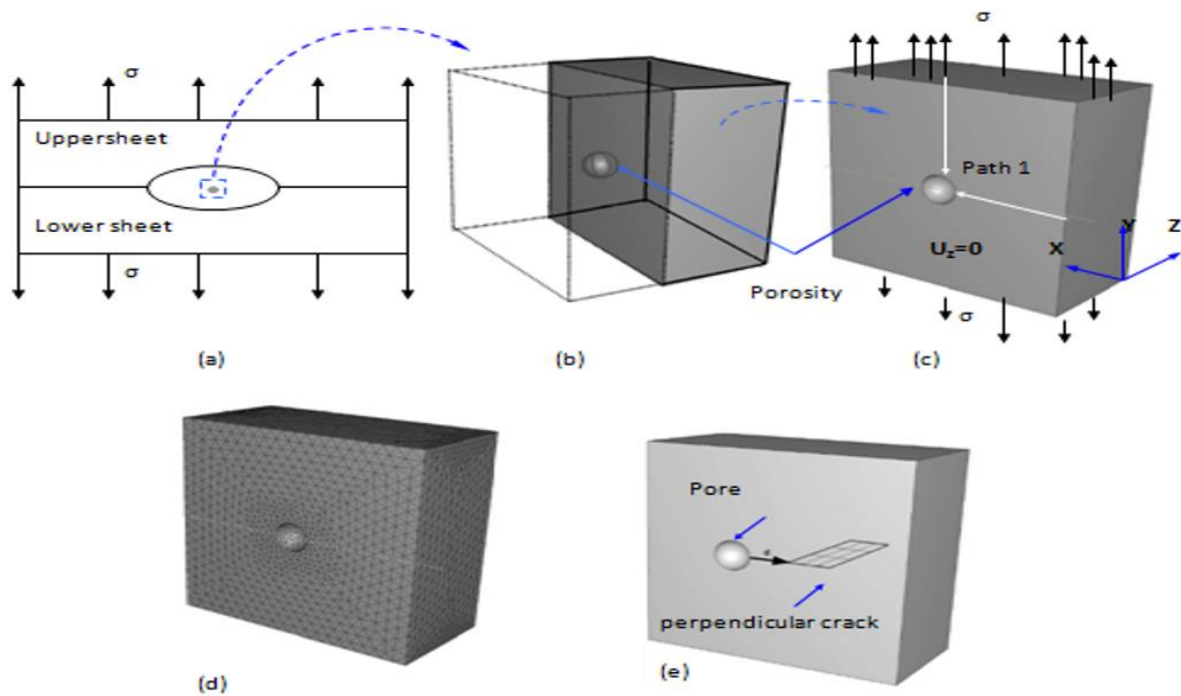


Figure 2. (a) 2-D schematic depiction of a welded joint with porosity, (b) the geometry of the entire model in a 3-D, (c) the geometry of one half of the complete model, boundary condition and loading condition, (d) the finite element mesh, and (e) the interaction of the pore-perpendicular crack [19]

The boundary and symmetry condition are: the z-axis displacement is set to zero ( $U_z=0$ ) (see Figure 2(c)). The length, width and thickness of the model are 350  $\mu\text{m}$ , 350  $\mu\text{m}$  and 175  $\mu\text{m}$ , respectively. On the other hands, the porosity is located in the centre of the weld nugget, and simulated as a hole with a diameter of 50  $\mu\text{m}$  [20]. It is expected that the solder joint's pores have a uniform distribution and size. Mechanics are used to load the latter (uniaxial traction).

A 4-node linear tetrahedron (C3D4) finite element model is chosen because the quality of the mesh surrounding the porosity has a significant impact on the accuracy of numerical calculation. The finite element model, which contains 47965 elements and a fine grid in the porosity, is depicted in Figure 2(d).

The material sample selected for this study was steel, considered as elastic material with a modulus of elasticity of

210 GPa and a Poisson's ratio of 0.3.

### 4. RESULTS AND DISCUSSION

#### 4.1 Effect of the mechanical load

In this study, the applied load  $\sigma_y$  is varied from 50 MPa up to 150 MPa. For each load applied, the Abaqus computer code gives the stress intensity factor values in opening mode and in shear mode. The intensity and distribution of the equivalent mechanical stresses in the model around the defect determine the lifetime of this structure.

The way that mechanical loads are distributed determines how long welded structures will last. The relationship between

mechanical loading and the amplitude and distribution of the Von Mises equivalent stress that is generated in the matrix along “path 1” (see Figure 2(c)) is shown in Figure 3. The level of the matrix peaks close to the interface of the pore, proving conclusively that greater effort causes greater stress.

#### 4.2 Crack behavior

In this section, we will take three mechanical loads, and we vary the length of the crack from 25  $\mu\text{m}$  up to 100  $\mu\text{m}$ . These values of the applied load are lower than the elastic limits of steel.

For each loading, one will determine the variation of the stress intensity factors in mode I and II according to the size of crack.

This section of the article analyzes the mechanical behavior of a fracture that starts in the matrix very near the pore. The fluctuation of the stress intensity variables in modes I and II is used to investigate this behavior. Several parameters’ effects have been researched. This research, which tries to investigate the behavior of cracks started in welded models, fits into that environment. A key factor in the commissioning and durability of a welded connection is the analysis of the stress intensity as a function of the interaction between two flaws (crack-pore) (see Figure 2(e)).

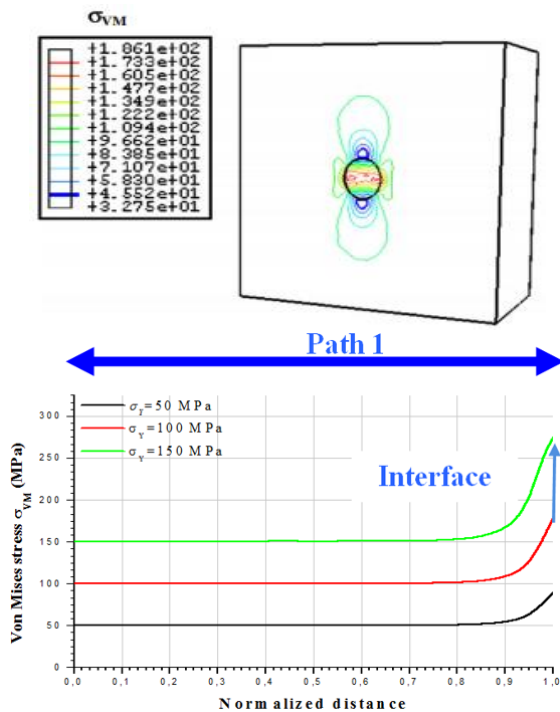


**Figure 3.** Variation in equivalent stress for path 1 in response to a mechanical loading for  $\Theta=50 \mu\text{m}$

##### 4.2.1 Effect of crack size

The size of a crack that starts in the matrix and is described by “a” in a location extremely close to the pore and perpendicular to the axis of the applied load is studied in relation to the stress intensity factor. Figure 4 illustrates how the crack length affects the stress intensity factor in modes I and II. The biggest load correlates to the bigger value of the  $K_I$  factor, demonstrating the proportionality between the factor  $K_I$  and the applied load. The matrix-pore and matrix-crack interfaces are where the greatest stresses are found. Figure 4(a)

demonstrates unequivocally how the growth of this mode I crack causes the stress intensity factor to rise.

Figure 4 illustrates how crack size affects the mode II stress intensity component (b). This graph demonstrates that when compared to the mode I stress intensity factor, the mode II stress intensity factor is negligible.

##### 4.2.2 Effect of porosity size

Figure 5 illustrates how pore size affects the stress intensity component. It demonstrates how an increase in pore size causes the stress intensity at the crack front to automatically rise. The stress intensity factor  $K_{II}$  is still at a low level.

##### 4.2.3 Effect of porosity form

In this instance, we investigated the impact of the defect’s shape on the development of the previously examined fracture. Figure 6 illustrates how the pore geometry affects the stress intensity factor. It demonstrates that the factor  $K_{II}$  is not directly impacted by pore geometry. There are, however, some variances in the factor  $K_I$ .

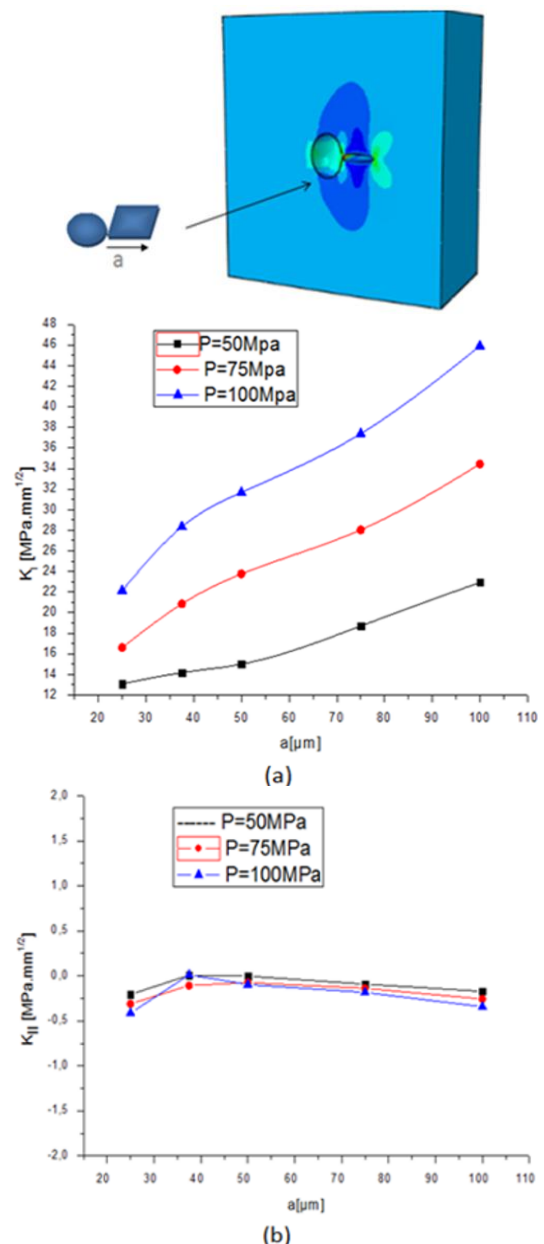


**Figure 4.** Changes in the stress intensity factor with respect to fracture length (a) ( $\Theta=50 \mu\text{m}$ )

#### 4.2.4 Effect porosity-crack interaction

In this part of the work, an analysis of the crack-porosity interaction effect on the stress intensity factor was conducted (Figure 2(e)). We will fix the dimensions of the structure, the size of the crack and the diameter of the pore. The diameter of the pore was taken equal to the size of the crack. We will vary the distance between these two defects.

The impact of pore-crack interaction on crack propagation has been examined in this section of the investigation. The fluctuation of the stress intensity factor as a function of the pore-crack distance (d) is depicted in Figure 7. It is clear that although the curve for the stress intensity factors  $K_I$  and  $K_{II}$  fluctuates, it essentially stays constant.

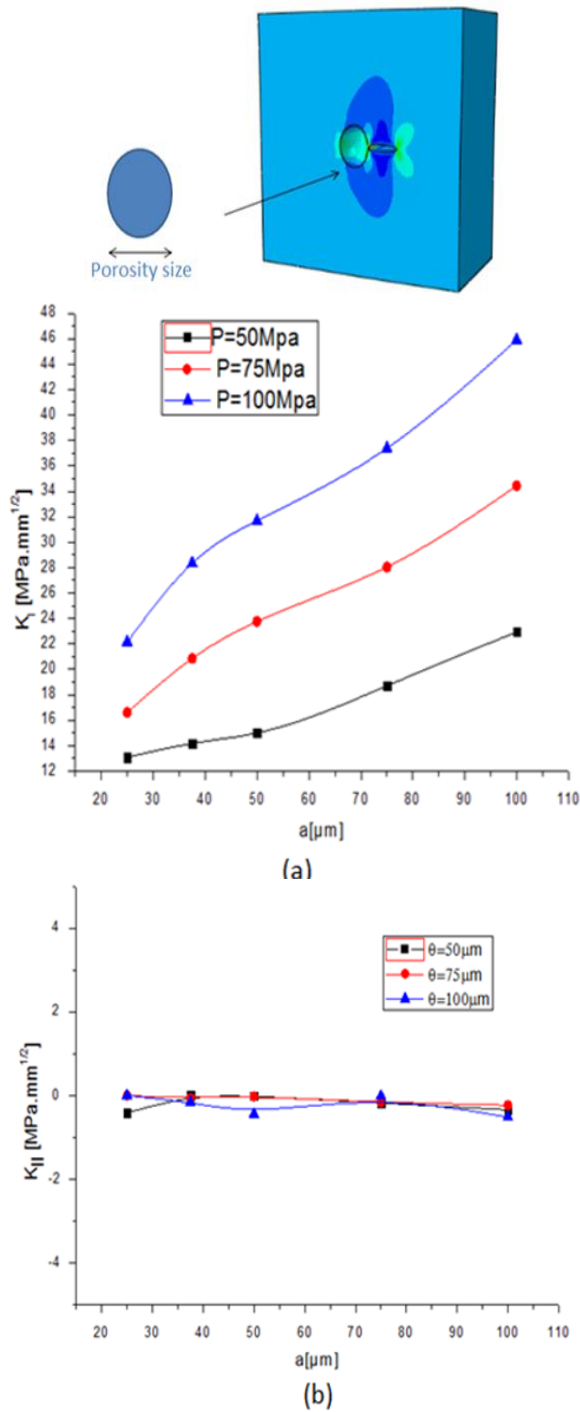


**Figure 5.** Changes in the stress intensity factor with respect to pore size ( $\Theta$ ) ( $\sigma_y=100$ MPa)

#### 4.2.5 Effect of the orientation of the crack

In this section, we will vary the orientation angle of the crack from  $0^\circ$  to  $120^\circ$ . We will fix the dimensions of the structure, the size of the crack and the diameter of the pore. For each orientation of the crack, one will determine the variation of the stress intensity factors in mode I and II.

The previously identified crack is pointed in the direction of the axis parallel to the applied load at an angle ( $\phi$ ) denoted by. The objective of this section of the work is to examine how the crack's orientation affects the ways in which it spreads. According to the crack's orientation angle, this forecasts the main mode of propagation. Figure 8 shows the outcomes that were thus produced. The crack's direction and the stress intensity factor in modes I and II are depicted in this figure. This fault in mode I is more likely to spread with this orientation, according to analysis of the figure. When it goes toward, this originally massive fissure grows weaker and weaker.

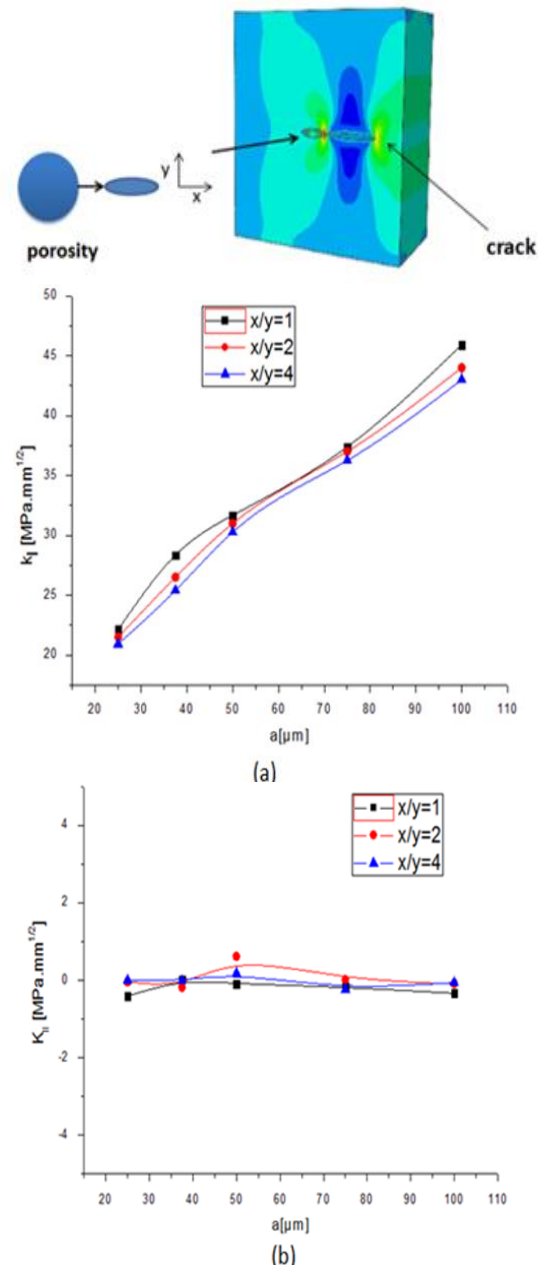
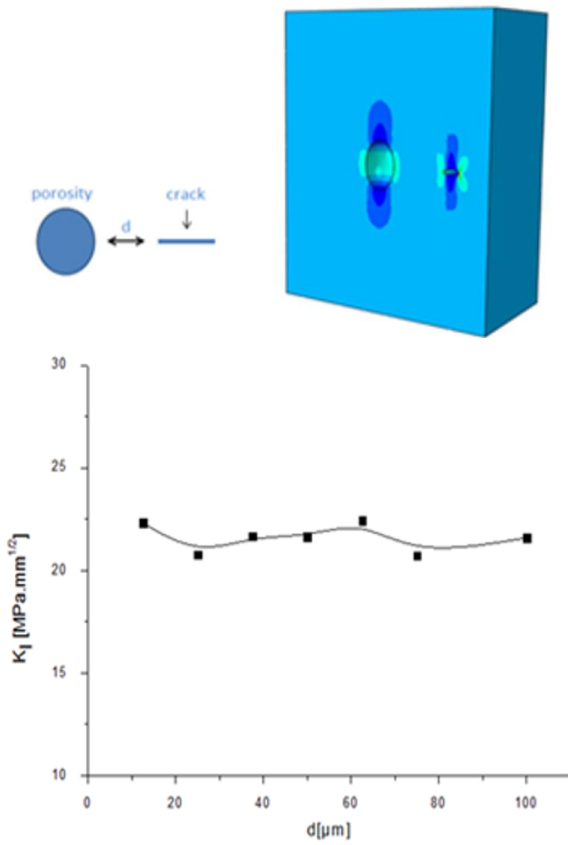
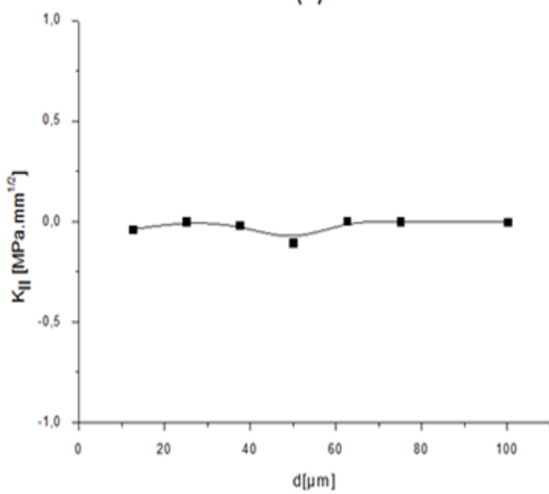


**Figure 6.** Changes in the stress intensity factor with respect to pore shape ( $\sigma_y=100$  MPa,  $\Theta=50$   $\mu$ m)



(a)



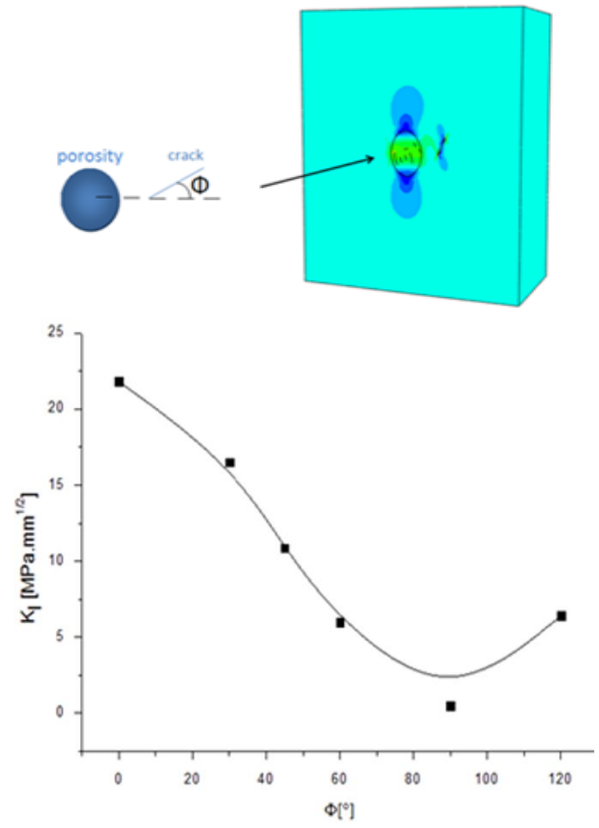
(b)

**Figure 7.** The relationship between the pore-crack distance and the variation of the stress intensity factor ( $\sigma_y=100$  MPa,  $\Theta=50$   $\mu\text{m}$ )

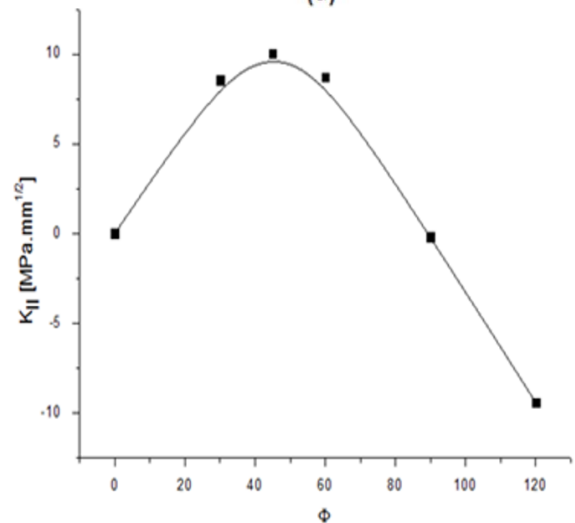
Figure 8(b) illustrates how the orientation of the fracture, which started perpendicular to the applied load, affects the fluctuation of the stress intensity component  $K_{II}$ . The stress intensity factor is sensitive to the location of the crack, as this figure demonstrates.

## 5. CONCLUSIONS

The study of the induced Von Mises stress distribution and the stress intensity factor in a ferritic matrix by defects resulting from the welding process has been addressed in this work.



(a)



(b)

**Figure 8.** Change in the stress intensity factor according to the crack's inclination angle ( $\sigma_y=100$  MPa,  $\Theta=50$   $\mu\text{m}$ )

A modeling by the finite element method is developed to analyze the failure behavior by the presence of porosity resulting from the welding process in a weld joint. The results of this study show that:

- ✓ The presence of porosities in the weld joint leads to a concentration of stresses.
- ✓ The level of the equivalent stress induced in the porous matrix increases with the increase in the intensity of the stresses applied. The distribution of pores in the ferritic matrix not only determines the mechanical resistance of the welded material, but also the amplitude of the local stresses induced in the weld joint in the close vicinity of this defect.

- ✓ A crack initiated in the plate perpendicular to the applied load propagates preferentially by opening. The values of  $K_I$  are much higher than those of  $K_{II}$ .
- ✓ The mode of opening is more significant than that of shearing. This factor is more important than the loading applied is more significant.
- ✓ The presence of localized porosity in the direction of propagation of a crack accelerates its growth kinetics. This acceleration is defined in terms of the intensification of the stress intensity factor. The porosity-crack interdistance determines the most dominant failure mode. A tendency of these two defects favors the mode of opening of this crack and a distance the mode of shearing.
- ✓ The stress intensity factor takes a high level when the porosity becomes spherical, this concentration increases rapidly and becomes increasingly weak. Thus, the acute porosities are less dangerous compared to the spherical ones.
- ✓ The mode of growth of a crack initiated in the vicinity of porosity depends on its orientation with respect to the direction of traction.

## REFERENCES

[1] Geslain, E. (2018). Resistance Welding of Coated Thin Sheets, Core Formation in an Assembly of Three Sheets. Lorient, France.

[2] Pierre, Y. (2021). What Is Spot Welding (and Is It Important). <https://weldingheadquarters.com>.

[3] Bouafia, F., Boutabout, B., Mecridi, M.A. (2009). Finite element analysis of the fracture behavior of welded structures by spot welding, *Matériaux, Techniques*, 97: 339-345. <https://doi.org/10.1051/Mattech/2009042>

[4] Bouafia, F., Boualem, S., El Amin, M.M., Benali, B. (2011). 3-D finite element analysis of stress concentration factor in spot-welded joints of steel: The effect of process-induced porosity. *Computational Materials Science*, 50(4): 1450-1459. <https://doi.org/10.1016/j.commatsci.2010.11.033>

[5] Ergun, E., Aslantaş, K., Tasgetiren, S., Topcu, M. (2006). Fracture analysis of resistance welded L-shaped and straight sheets. *Materials and Design*, 27(1): 2-9. <https://doi.org/10.1016/j.matdes.2004.09.013>

[6] Dassaut Systèmes Simulia Corp-Abaqus/CAE 6.11 User's Manual. Available at: <https://www.3ds.com/products-services/simulia>.

[7] Spitsen, R., Kim, D., Flinn, B., Ramulu, M., Easterbrook, E.T. (2005). The effects of post-weld cold working processes on the fatigue strength of low carbon steel resistance spot welds. *Journal of Manufacturing Science and Engineering*, 127(4): 718-723. <https://doi.org/10.1115/1.2034514>

[8] Moroni, F., Pirondi, A., Kleiner, F. (2010). Experimental analysis and comparison of the strength of simple and hybrid structural joints. *International Journal of Adhesion and Adhesives*, 30(5): 367-379. <https://doi.org/10.1016/j.ijadhadh.2010.01.005>

[9] Zhao, Z.L., Yang, J.G., Liu, X.S., Fang, H.Y. (2008). Numerical simulation of basal parameters for fatigue evaluation of electromotor rotor welded structure. In *Materials Science Forum*, 575-578: 643-648. <https://doi.org/10.4028/www.scientific.net/MSF.575-578.643>

[10] Golestaneh, A.F., Ali, A. (2009). Application of

numerical method to investigation of fatigue crack behavior through friction stir welding. *Journal of Failure Analysis and Prevention*, 9: 147-158. <https://doi.org/10.1007/s11668-009-9210-9>

[11] Wang, P.C., Ewing, K.W. (1991). Fracture mechanics analysis of fatigue resistance of spot welded coach-peel joints. *Fatigue and Fracture of Engineering Materials and Structures*, 14(9): 915-930. <https://doi.org/10.1111/j.1460-2695.1991.tb00725.x>

[12] Adib, H., Gilgert, J., Pluvinage, G. (2004). Fatigue life duration prediction for welded spots by volumetric method. *International Journal of Fatigue*, 26(1): 81-94. [https://doi.org/10.1016/S0142-1123\(03\)00068-9](https://doi.org/10.1016/S0142-1123(03)00068-9)

[13] Pan, N., Sheppard, S. (2002). Spot welds fatigue life prediction with cyclic strain range. *International Journal of Fatigue*, 24(5): 519-528. [https://doi.org/10.1016/S0142-1123\(01\)00157-8](https://doi.org/10.1016/S0142-1123(01)00157-8)

[14] Radaj, D., Zhang, S. (1992). Stress intensity factors for spot welds between plates of dissimilar materials. *Engineering Fracture Mechanics*, 42(3): 407-426. [https://doi.org/10.1016/0013-7944\(92\)90163-9](https://doi.org/10.1016/0013-7944(92)90163-9)

[15] Fekirini, H., Serier, B., Bouafia, F., Bouiadjra, B.A.B., Hayat, S.S., Bouafia, S.A. (2012). Effect of precipitate-precipitate interaction on residual stress in welded structure. *Computational Materials Science*, 65: 207-215. <https://doi.org/10.1016/j.commatsci.2012.06.005>

[16] Souad, S., Serier, B., Bouafia, F., Boudjra, B.A.B., Hayat, S.S. (2013). Analysis of the stresses intensity factor in alumina-Pyrex composites. *Computational Materials Science*, 72: 68-80. <https://doi.org/10.1016/j.commatsci.2013.01.030>

[17] Bouafia, F., Serier, B., Serier, N., Hayat, S.S. (2014). Effect of density and pointed corner degree of pore on local stress in welded structures: Defect in marine structures. *International Scholarly Research Notices*, 2014:834659. <https://doi.org/10.1155/2014/834659>

[18] Farida, B., Hadid, L., Boualem, S., Sikandar, S. (2020). Finite element analysis of the interface defect in ceramic-metal assemblies: Alumina-Silver. *Frattura ed Integrità Strutturale*, 14(53): 1-12. <https://doi.org/10.3221/IGF-ESIS.53.01>

[19] Bouafia, F., Serier, B., Boutabout, B., Bouiadjra, B.A.B. (2011). Numerical analysis of the effect of pore on local stresses in spot welds. *Computational Materials Science*, 50(8): 2517-2529. <https://doi.org/10.1016/j.commatsci.2011.03.036>

[20] Dorlot, J. M., Bailom, J.P., Masounave, J. (1985). *Book of Materials*. Polytechnique of Montréal, Quebec, Canada.

## NOMENCLATURE

SIF	stress intensity factor
FEM	finite element method
J	the integral
k	coefficient of stress intensity factor Mpa.mm <sup>1/2</sup>
t	Thickness
a	the size of a crack, μm
d	the pore-crack distance, μm

## Greek Symbols

σ	radial normal stresses, Mpa
---	-----------------------------

$\phi$  the orientation of the crack, ( $^{\circ}$ )  
 $\Theta$  The pore size,  $\mu\text{m}$

**Indices**

I opening mode (mode I)

II sliding mode (mode II)  
i inner  
o Outer  
u Upper  
l Lower